ACS OMEGA

http://pubs.acs.org/journal/acsodf

Article

Excitation-Dependence of Excited-State Dynamics and Vibrational Relaxation of Lutein Explored by Multiplex Transient Grating

Liping Lu, Yunfei Song, Weilong Liu, and Lilin Jiang*

Cite This: *ACS Omega* 2022, 7, 48250−48260

Read Online

ACCESS | Metrics & More | Article Recommendations | Supporting Information

ABSTRACT: Multiplex transient grating (MTG) spectroscopy was applied to lutein in ethanol to investigate the excitation-energy dependence of the excited-state dynamics and vibrational relaxation. The transient spectra obtained upon low (480 nm) and high-energy (380 nm) excitation both recorded a strong excited-state absorption (ESA) of $S_1 \rightarrow S_n$ as well as a broad band in the blue wavelength that was previously proposed as the S* state. By means of Gaussian decomposition and global fitting of the ESA band, a long-time component assigned to the triplet state was derived from the kinetic trace of 480 nm excitation. Moreover, the MTG signal with a resolution of 110 fs displayed the short-time quantum beat signal. In order to unveil the vibrational coherence in the excited-state decay, the linear and non-linear simulations of the steady spectrum and dynamic signals were presented in which at least three fundamental modes standing for C−C stretching (ν_1), C═C stretching (ν_2), and O−H valence vibrations (ν_3) were considered to analyze the experimental signals. It was identified that the vibrational coherence between ν_1 and ν_3 or ν_2 and ν_3 was responsible for quantum beat that may be associated with the triplet state. We concluded that upon low- or high-energy excitation into the S_2 state, the photo-isomerization of the molecule and structural recovery on the time-scale of vibrational cooling are the key factors to form a mixed conformation in the hot-S_1 state that is the precursor of a long life-time triplet.

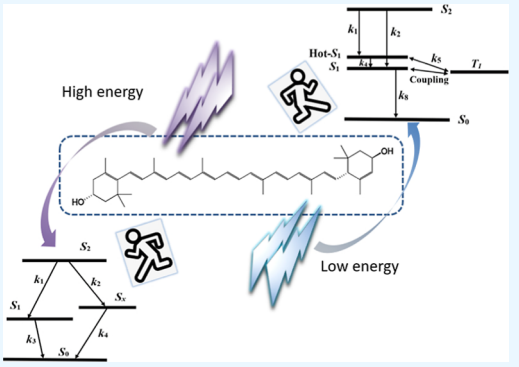

1. INTRODUCTION

Carotenoids are widely distributed pigments that perform multiple physiological functions in the biological systems due to the complex properties of lowest-lying excited states and vibrational relaxation.[1,2] The crucial functions of carotenoids in photosynthesis organisms are all related to the energy deactivation network, ranging from photoprotection against oxidative damage through quenching of triplet chlorophyll phosphorescence to assistant light harvesting by absorbing light energy and transferring it to chlorophylls.[3−7] Therefore, the very complicated excited-state structure, vibrational relaxation, and resulted energy-decay pathway have been the topics of experimental and theoretical studies. The most popular paradigm so far for the carotenoids photo dynamics consists of one ground state and two low-lying excited states: S_0, S_1, and S_2 corresponding $1A_g^-$, $2A_g^-$, and $1B_u^+$ symmetry, respectively, with energy from low to high.[6,8,9] Direct one-photon excitation into S_2 is strongly allowed, while into S_1 is highly forbidden due to the symmetry-allowed selection rule. Thus, the characteristic linear absorption of carotenoids in blue-green wavelength originates from $S_0 \rightarrow S_2$ transition.

The well-defined three-state paradigm of carotenoids previously discussed is useful for a basic description of excited-state dynamics of conjugation lengths $N = 7-9$. It turns out that carotenoids with $N > 10$ have other low-lying dark states around S_1 which are supposedly involved in energy-relaxation pathways.[10,11] However, the assignment of these "dark" excited states that have been revealed in some literature in order to illustrate the particular transient spectra is still a matter of debate.[12−14] The most discussed dark state labeled S* was first reported for long synthetic β-carotene homologues as a hot-ground state[15] and then re-described in detail as an excited state in spirilloxanthin solution and protein-spirilloxanthin bounded complexes based on the femtosecond transient absorption (TA).[16] After that, it was subsequently observed in other bacterial light harvesting proteins.[17] Currently, reports have shown that the S* had multiple origins, both from excited and ground states.[18] However, the exact origin of S* remains a subject of debate. In 2003, Larsen proposed a new dark state $S^‡$ assigned to β-carotene that was only observed in transient signals initiated via high-energy excitation photons (400 nm), not via lower-energy photons (500 nm).[19] It was concluded that the dynamic feature of S* and $S^‡$ states described by a distinct shoulder in the high-energy and low-energy side of the

Received: October 3, 2022
Accepted: November 28, 2022
Published: December 16, 2022

$S_1 \rightarrow S_n$ transition respectively usually has a longer lifetime than the S_1 state.[14] In recent years, many experiments reveal the appearance of long-lived excited state S* as a carotenoid triplet originating from singlet fission that has been the hot-research topic owing to the great potential in photovoltaic materials.[19−23] Although extensive research during the past few years shed some light on the possible origin of the S* state, none of the hypotheses, the S* being either a separate electronic excited state or a hot-ground state, has yet been proven so far.

In the framework of femtosecond pump−probe spectroscopy, the S_2 state relaxes rapidly within 300 fs to the optically forbidden S_1 state by internal conversion.[24] Subsequently, the S_1 state decays to the ground state S_0 with a lifetime from 1 to 100 ps depending greatly on the conjugation length of the carotenoids.[8] The non-radiative relaxation of $S_2 \rightarrow S_1 \rightarrow S_0$ involves other intermediate dark state such as S* as well as vibrational coupling. The details of the intermediate state which was assumed to originate from a separate electronic state or a twisted S_2 state are unclear.[18] As a result, besides the population dynamics of excited states, the vibrational relaxation is another critical issue to investigate the energy inactivation of carotenoids. Some research suggested the possibility of carotenoid-chlorophyll energy transfer occurring from hot-vibration states of the carotenoid S_1 in the LHCII protein[25,26] that makes a deeper understanding of the vibrational relaxation dynamics very important. Obviously, during the excited-states relaxation a carotenoid molecule will carry an appreciable amount of excess vibrational energy, which may be probed by the time-dependent spectral changes due to vibrational relaxation.[27] A thorough understanding of the excited-state decay and corresponding vibrational relaxation remains contradictory, although a vast number of investigations have been carried out over the last two decades.

Many powerful spectroscopic techniques with both high time and wavelength resolution have been successfully applied to investigate the excitation energy flow within the complicated electronic manifolds of carotenoids. TA spectroscopy has shown great power in probing the population dynamics. Other multidimensional time-resolved technique [pump−dump−probe,[28,29] transient grating (TG)] measurements allow one to investigate the evolution of vibrational coherence in electronic states.[30] In a traditional TG, time coincident laser pulses with the same frequency are crossed into the sample. The time-dependent diffraction signal provides a real-time access to the dynamic process induced by the excitation pulses. Multiplex TG (MTG) spectroscopy using white light continuum as a probe light provides better sensitivity than TA because of the free-background nature.[31,32] The population dynamics and vibrational coherence processes after excitation of two initial pulses can be probed by a third time-delayed continuum once and for all.

MTG can be used to analyze a wide variety of physicochemical properties in various systems, such as excitation energy, triplet quantum yield, and vibrational relaxation dynamics. In this study, we addressed in particular the MTG experiment signal of lutein together with simulation of a non-linear signal to investigate these dark states of carotenoid. We also compared the excited state decay and the vibrational relaxation upon visible (480 nm) and ultraviolet excitation (380 nm) in this work. The results demonstrate that the excited-state absorption (ESA) follows the same spectral profile described previously. By means of Gaussian decomposition and global fitting of experimental ESA signal, we are able to confirm the properties of excited-state dynamics in which a long-time component of triplet state is found. On the other aspect, we extract the quantum beats from kinetic trace of 20 fs step MTG signal by subtracting the population dynamics. In the frame of non-linear response theory, at least three vibrational modes are needed to simulate the steady and TA spectra. Last, we discuss the excitation-dependence of long-lived excited state of lutein.

2. EXPERIMENTAL SECTION

All-*trans* lutein ($C_{40}H_{56}O_2$, 92%) was provided by Shanghai Yuanye Biotechnology Co. Ltd. Lutein was dissolved in ethanol of analytical grade to achieve monomer samples with a concentration of 35 μM for lutein. UV−vis absorption spectra in the range of 300−600 nm were checked with a Shimadzu UV-1700 spectrophotometer to ensure the monomer solution. The sample in a 1 mm cuvette had a maximal absorbance of ∼0.5 and the absorbances of 380 and 480 nm were 0.161 and 0.371, respectively.

The details of experimental apparatus of MTG have been previously described.[32] Briefly, the setup employs a regenerative Ti: sapphire amplifier (Spitfire, Spectra Physics) as the primary beam source. The output pulse (100 fs, 1 kHz, 800 nm) was split into two beams via a beam splitter (90 and 10%). The 90% beam pumped an optical parametric amplifier (OPA, OPA-800FC, Spectra Physics) to produce a pulse with a wavelength centered at 480 (2.3075×10^{15} photons/cm^2/pulse) and 380 nm (1.8267×10^{15}photons/cm^2/pulse), which was split into two equal beams. These beams were used as the pump pulse for the MTG studies. The 10% beam was focused via a lens on the water to produce a white-light continuum, which was used as the probe pulse. In the experiments, the relative polarization of the pump and probe beams was set to the magic angle (54.7°). The energy of the pump pulse was about 300 nJ, while the energy of probe pulse was less than 100 nJ. To avoid damage to the sample, a cuvette with an optical pathlength of 1 mm was mounted on a translation stage with the appropriate speed. The full width at half-maximum (fwhm) of the pump and probe pulse cross-correlation of the samples was approximately 110 fs, which represented the time resolution of the TG experiment. However, in order to improve the fitting precision to the experimental curves, the probe pulse was scanned with a step of 20 fs. The description of spectral correction was shown in the previous literature.[33] All the measurements were carried out at room temperature in the dark room.

3. SIMULATION OF MTG SIGNAL

In the perturbation theory of the filed-matter interaction, Hamiltonian operators acting on the system N times create a N-order polarization $P^{(N)}(t)$ which relates the optical response function $R(t_1, t_2, t_3)$ to the driving field $E(t)$.[34] The response function can be described by a line-broadening function $g(t)$ resulted from a time-dependent correlation function $M(t)$. Once the line-broadening function is given, all linear or nonlinear signals can be calculated. To account for bath and vibrational effects in the excitation processes, two models are included. First, the influence of the bath is expressed by Brownian oscillator spectral density components during the evolution in electronic states. For this purpose, we introduce the line-shape function $g_s(t)$ of Brownian oscillator in the high-

https://doi.org/10.1021/acsomega.2c06371
ACS Omega 2022, 7, 48250−48260

temperature limit to perform a simplified model calculation of the MTG signal. Second, to integrate vibrational effects in the decay processes, an underdamped oscillation is used to produce the line-broadening function $g_v(t)$[35]

$$g_s(t) = \left(\frac{\Delta^2}{\Lambda^2} - i\frac{\lambda}{\Lambda}\right)(\exp(-\Lambda t) + \Lambda t - 1) \tag{1a}$$

$$g_v(t) = \sum_i \sum s_i \left\{ \coth\left(\frac{\omega_i}{2kT}\right)[1 - \cos(\omega_i t)] + i[\cos(\omega_i t) - \omega_i t] \right\} \tag{1b}$$

$g_s(t)$ shows the broadening effect of solvent, where Δ is the coupling strength with solvent bath, λ is the reorganization energy $\lambda = \frac{\Delta^2}{2kT}$, and Λ is the attenuation rate of bath fluctuation. $g_v(t)$ indicates spectral line of vibrational modes, in which s_i is Huang–Rhys factor (electron–phonon coupling strength) of ith electron–vibration coupling and ω_i is the frequency of the ith molecular vibrational mode. The total line-broadening function is the sum of $g_s(t)$ and $g_v(t)$. Next, the steady absorption coefficient can be expressed in terms of linear response function. For a two–level system, the linear absorption of molecule is.[36]

$$A(\omega) \propto \mathrm{Re} \int_0^\infty \mathrm{d}t \exp[i(\omega - \omega_{eg})t - g(t)] \tag{2}$$

Here, $g(t)$ is the line-shape function containing vibration and solvent contribution. ω_{eg} is central absorption as a parameter. We used the linear absorption formula of eq 2 to fit the steady absorption spectrum in the experiment based on the least square method and obtained full agreement (Figure 8).

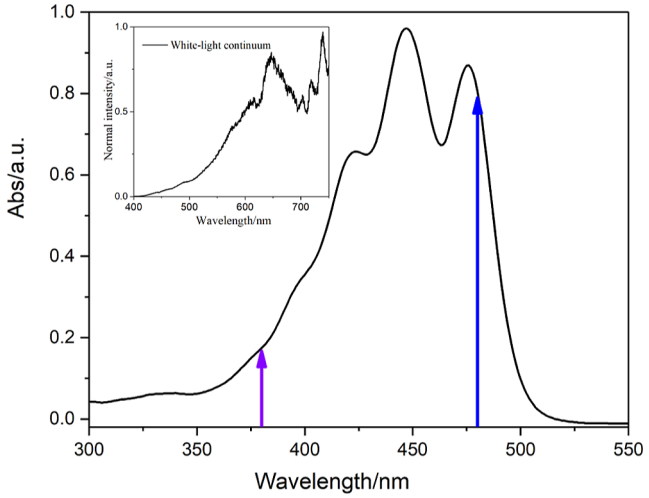

Figure 1. Steady absorption of lutein in ethanol. The probe white-light continuum used in MTG is shown on the top of the figure. The blue and purple arrows are the excited pulses in MTG.

For the nonlinear signal, the response functions are introduced to describe the MTG transient signal which can be classified by their rephasing or non-rephasing properties. In our experiment, the signal along the phase-matched direction of $-k_1 + k_2 + k_3$ is assigned to rephasing type and the relative excitation processes are SE, GSB, and ESA shown with double-sided Feynman diagrams in Figure 7 corresponding to response functions of R_1, R_2, and R_3. We ignore the population dynamics and just investigate the vibrational relaxation; then, the exact response functions are in principle using the following expression.[35,37,38]

$$R_1 = \exp[i\omega_{\bar{2}\leftarrow\bar{0}}(t_1 - t_3)]\exp[-\Gamma_2(t_1 + t_3)] \exp[-g^*(t_1) + g^*(t_2) - g(t_3) - g^*(t_1 + t_2) - g^*(t_2 + t_3) + g^*(t_1 + t_2 + t_3)] \tag{3a}$$

$$R_2 = \exp[i\omega_{\bar{0}\leftarrow\bar{2}}(t_1 - t_3)]\exp[-\Gamma_2(t_1 + t_3)]\exp(-k_{\bar{1}\leftarrow\bar{2}}t_2) \exp[-g^*(t_1) + g(t_2) - g^*(t_3) - g^*(t_1 + t_2) - g(t_2 + t_3) + g^*(t_1 + t_2 + t_3)] \tag{3b}$$

$$R_3 = \exp(i\omega_{\bar{0}\leftarrow\bar{2}}t_1 - i\omega_{n\leftarrow\bar{1}}t_3)\exp(\Gamma_2 t_1 - \Gamma_1 t_3)\exp(-k_{\bar{0}\leftarrow\bar{1}}t_2) \exp[-g^*(t_1) - g(t_2) - g(t_3) + g^*(t_1 + t_2) + g(t_2 + t_3) - g^*(t_1 + t_2 + t_3)]\exp[g(t_2) - 2g(t_3) - g^*(t_1 + t_2) - g(t_2 + t_3) + g^*(t_1 + t_2 + t_3) - g(t_3)] \tag{3c}$$

Here, t_1 is the time interval of the first and second pulse, t_2 is the time interval of the second pulse and third prob light, and t_3 is signal-collecting time. For the MTG $t_1 = 0$ is setup. Both Γ_1 and Γ_2 are set to zero to exclude the contribution of population. In the impulsive limit, the MTG signals are simply given by the time integration of the total response function. We assume the pulse for a δ function; then, the non-linear signal is

$$S_{MTG}(t_1, t_2) = \int_0^\infty |R_1 + R_2 + R_3|^2 \mathrm{d}t_3 \tag{4}$$

4. RESULTS AND DISCUSSION

4.1. Steady-State Absorption. The overall one-photon absorption spectrum of lutein in ethanol is shown in Figure 1 with a typical shape in the 300–550 nm region that is associated with the strongly allowed $S_0 \rightarrow S_2$ transition. The steady absorption exhibits a characteristic three-peak profile due to the vibrational structure of S_2 whose details will be discussed later. In ethanol, besides the vibrational peaks located at 476 (0–0), 447 (0–1), and 423 nm (0–2), respectively, a weaker absorption band that covers the 200–350 nm spectral region is assigned to the $2B_u$. The positions of blue and purple arrows are the excitation wavelength (480 and 380 nm) of MTG. The white continuum of probe light is shown on the top of Figure 1

4.2. TA of $S_1 \rightarrow S_n$. MTG signal has the zero background and the intensity I_{TG} is superior sensitive to the molecular population and vibration dynamics for it is proportional to the square of concentration of the transient species formed during the photoinduced populations,$I_{TG} \propto (\Delta A)^2$; nevertheless, it is typically difficult to analyze the spectra in the first few hundred femtoseconds due to the optical Kerr effect from the solvent.[39] As shown in supplement Figure S1, the initial signal from ethanol overlaps with the ground bleach and excited emission of carotenoids in the range of 400–450 nm which makes it impossible for us to distinguish the population signal of lutein from background. Therefore, we just focus on the ESA signal. Figure 2 shows the smoothed TA of ESA spectra of lutein

https://doi.org/10.1021/acsomega.2c06371
ACS Omega 2022, 7, 48250–48260

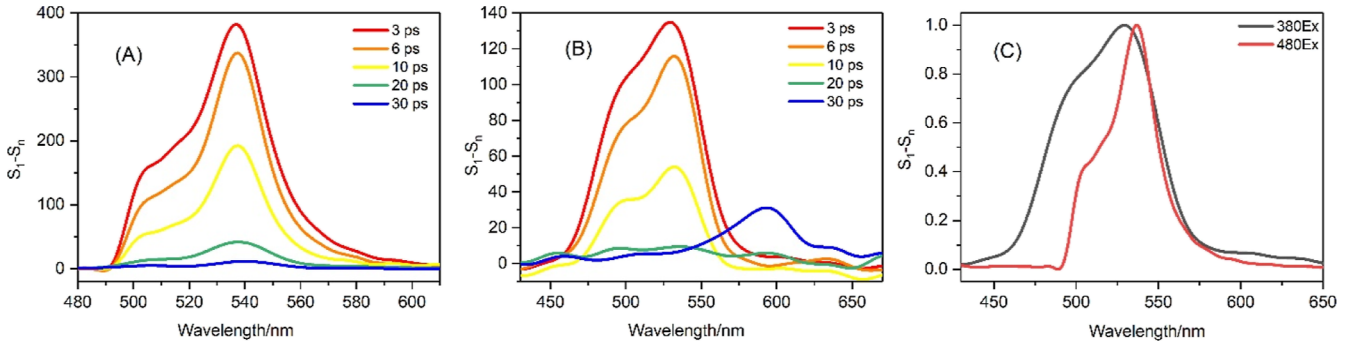

Figure 2. ESA of $S_1 \rightarrow S_n$ of lutein in ethanol taken at different time-delays. The wavelengths for excitation were chosen as 480 nm (A) and 380 nm (B) to excite the lowest and highest vibrational band of the S_2 state. The two ESAs both with 3 ps delay normalized to the maximum are compared (C).

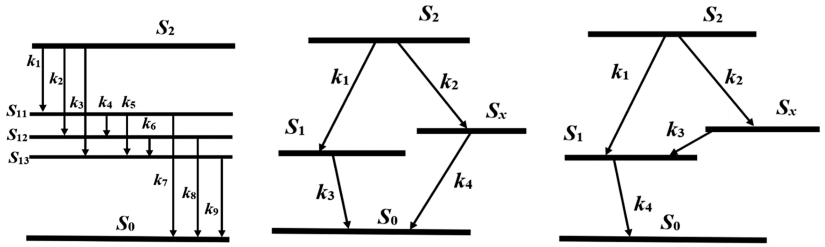

Figure 3. Three hypothetical schemes for the exploration of excited-state properties and dynamics of lutein. Scheme 1 (A) is established for 480 nm excitation with all possible internal conversions. Schemes 2 (B) and 3 (C) are used to describe the dynamics of 380 nm excitation, where the ESA of S_x can be fitted by one Gaussian curve.

solution excited by 480 (A) and 380 (B) nm in the 450−650 nm spectral window. At 480 nm, the lowest vibrational band of the S_2 state is selectively excited, while 380 nm is the higher energy excitation in the UV absorption range of S_2 state. Because the relaxation of the S_2 state occurs in range of 100−300 fs, most populations of lutein molecules are in the S_1 or other adjacent states at the arrival of detecting light with chosen time-delay. At these time-delays, the measured signals are dominated by $S_1 \rightarrow S_n$ absorption (ESA).

The experimental ESA (Figure 2) of Lutein in ethanol excited initially by two simultaneous pulses is analogous to that of carotenoid fucoxanthin in ethanol by one-photon excitation.[40] Regardless of the excited energy, Figure 2A,B displays a strong main peak corresponding to the $S_1 \rightarrow S_n$ absorption and a pronounced absorption shoulder band on the high-energy side of the main band, which is attributed to the transition from so called S* to a higher-lying excited state S_n.[19,41] In both cases, the ESA band reaches maximal value at about 3 ps time-delay and seemingly decreases to zero within 30 ps. However, a new band in Figure 2B is observed at 30 ps time-delay which may be associated to $S^{\ddagger}$ state or vibrational state.[42] The ESAs of 3 ps delay excited by 380 and 480 nm are contrasted in Figure 2C. In order to compare the transient spectra quantitatively, they are normalized at the maximal peaks. Although two ESA bands of different excitation are almost in the same shape, the main peak of the $S_1 \rightarrow S_n$ band for 380 nm excitation is 529 that blue shifts by 7 nm compared with 480 nm excitation that are in agreement with the previously published reports.[43,44] In addition to the spectral shift, the distinct shoulder for 380 nm excitation shows a broader absorption profile (fwhm: 70 nm) than 480 nm excitation (fwhm: 36 nm). Moreover, the absorption intensity ratio $\frac{I_{Sh}}{I_{Max}}$ of the blue shoulder to main band of 380 nm excitation is twice (0.8) that of 480 nm excitation (0.4). These spectral characteristics of the excitation-energy-dependent $S_1 \rightarrow S_n$ band can be explained by vibrational relaxation of S_1 in carotenoids following excess energy excitation and are supposed to be related to the excited-state dynamics and vibrational relaxation in S_1.[30,45]

To gain more insights into the S_1 exited state of lutein, all the spectra in Figure 2 are decomposed by several Gaussian curves shown in Figure S2 and in Table 1. In order to satisfactorily fit the ESA of 480 nm excitation, three Gaussian curves with peaks at about 536, 513, and 502 nm, respectively, are needed. While for 380 nm excitation, the ESA is fitted well only by two Gaussian peaks at about 533 and 498 nm. Based on the results of Gaussian decomposition of $S_1 \rightarrow S_n$ absorption band, three hypothetical schemes for the excited-state model of lutein in ethanol are proposed in Figure 3. Scheme 1 is used to describe the ESA of 480 nm excitation where the S_1 band is formed via three branched excited states whose properties will be identified further by global fitting. For ESA of 380 nm excitation, we assume a S_x state (Scheme 2 and Scheme 3) to account for one blue shoulder of Gaussian peak and investigate whether the two decay pathways are independent.

4.3. Population Dynamics of the Excited States. As evident in the typical TG spectra of Figure S3, some distinct features can be found from the dynamic curve: a sharp coherent spike at certain time due to the wave packet motion, an exponential decay with a slow time constant up to tens of picoseconds corresponding to the population relaxation, oscillatory contribution to the signal that can be used to investigate the role of vibrational mode. In 480 nm excitation,

https://doi.org/10.1021/acsomega.2c06371
ACS Omega 2022, 7, 48250−48260

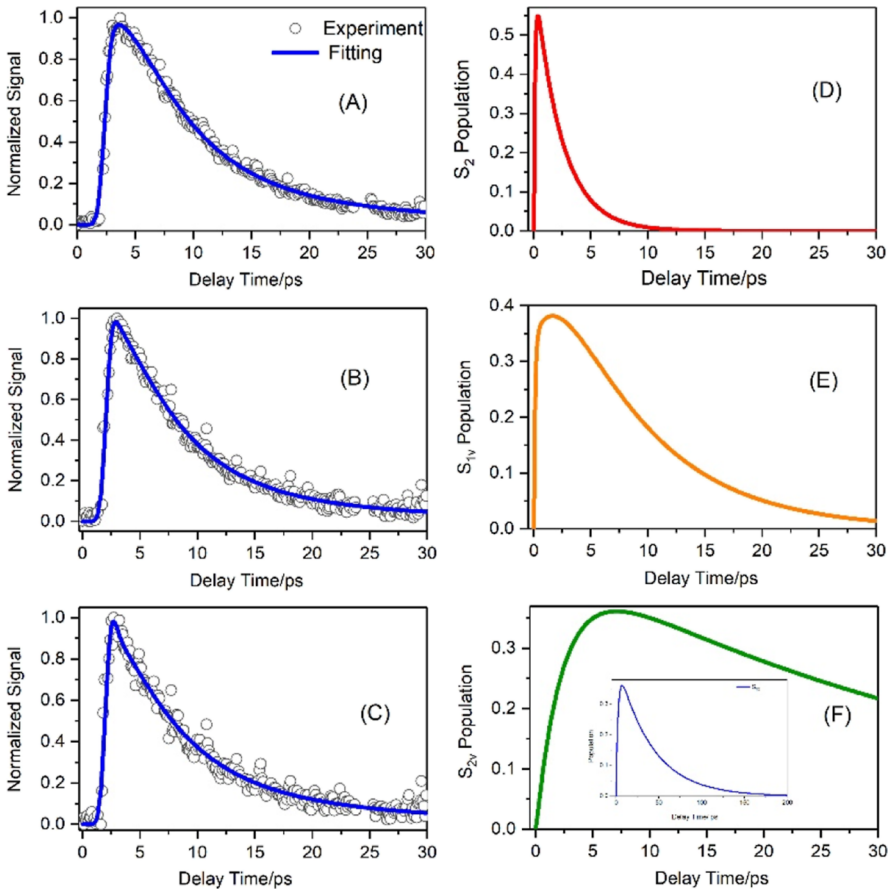

Figure 4. MTG kinetic trace (open circle) of lutein of 480 nm excitation corresponding 536, 516, and 502 nm ESA after 3 ps delay (the coherent spike of each curve has been cut off). The blue solid line is the best fitting curve from eq 6 with the errors of residual RMS 0.0244, 0.0314, and 0.0422 for (A−C) where the exponential decay is convoluted with instrumental response function. (D−F) are the three population equations of N_{11}, N_{12}, and N_{13}, respectively, based on scheme 1. The inserted figure is the population N_{13} of whole-time scope.

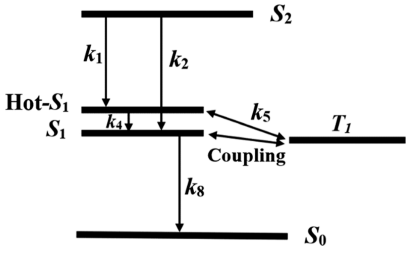

Figure 5. Reconstructed scheme 1 for excited-state dynamics of lutein in ethanol with 480 nm excitation. The lifetimes of S_2, Hot-S_1, S_1, and T_1 states are 106 fs, 2.8, 12, and 49 ps, respectively. The triplet state T_1 of 49 ps is coupling with S_1 state. The relaxation rate from hot-S_1 to T_1 is twice as fast as to S_1.

we also observe the Raman resonance signal (Figure S3A). In order to simplify the calculated procedure, the coherent spike of each curve has been truncated as the population is much weaker than the spike. Although, MTG could not record the S_2 dynamics due to the ethanol signal in the initial time, all population relaxation can be analyzed by a global fitting, which enables us to clearly visualize the evolution of the excited states. Notably, we used the square of the model population to fit the transient signal (eq 5a) by the least-square method, so as to obtain the reasonable parameters. For 480 nm excitation, four rate equations are determined according the Scheme 1 in Figure 3.

$$\frac{dN_2}{dt} = -(k_1 + k_2 + k_3)N_2 \tag{5a}$$

$$\frac{dN_{11}}{dt} = k_1N_2 - (k_4 + k_5 + k_7)N_{11} \tag{5b}$$

$$\frac{dN_{12}}{dt} = k_2N_2 + k_4N_{11} - (k_6 + k_8)N_{12} \tag{5c}$$

$$\frac{dN_{13}}{dt} = k_3N_2 + k_5N_{11} + k_6N_{12} - k_9N_{13} \tag{5d}$$

Then, the time-dependent population dynamics of each state can be obtained by solving this set of rate equations where N is the population and k is the relaxation rate between two states. The rate equations for Schemes 2 and 3 together with their solved population equation are shown in the supplement. Using the nonlinear least-squares method, the experimental kinetic signal $S(t)$ of MTG is fitted by the iterative convolution of the instrument response function and exponential decay function of population obtained by solving the rate equation. The instrument response function is put into the supplement.

$$S(t) \propto (A_1N_2 + A_2N_{11} + A_3N_{12} + A_4N_{13})^2 \tag{6}$$

In eq 6, A is the parameter of the contribution of each excited state to the MTG signal. The best fitted results and excited-state relaxation constant obtained from fitting the experimental signal are shown in Figure 4 and Table 2. In

https://doi.org/10.1021/acsomega.2c06371
ACS Omega 2022, 7, 48250−48260

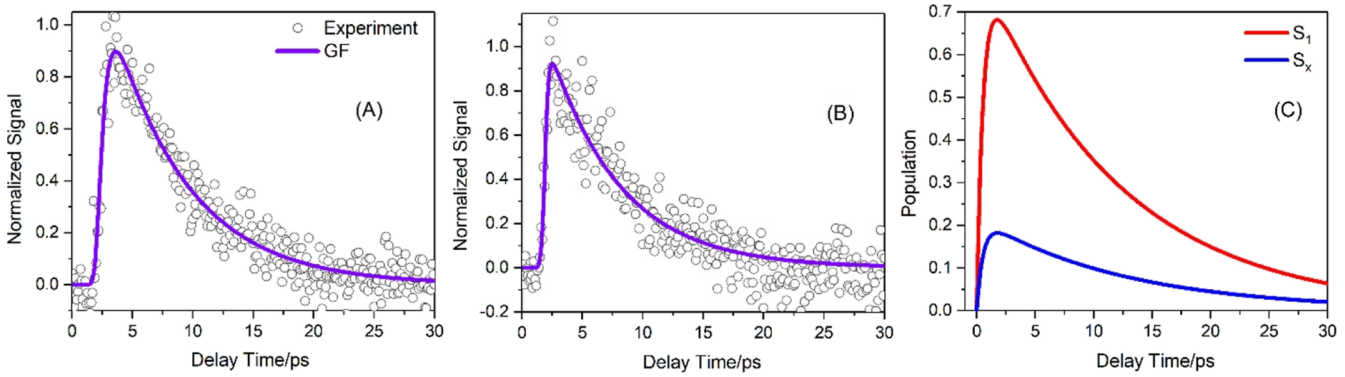

Figure 6. MTG kinetic trace (open circle) of 380 nm excitation. The purple curves are the fitted dynamics at 535 (A) and 494 nm (B) excitation with the errors of residual RMS 0.0737, 0.102, respectively. (C) is the calculated dynamics of S_1 and S_x based on Scheme 2 with lifetimes 14.9 and 14 ps, respectively.

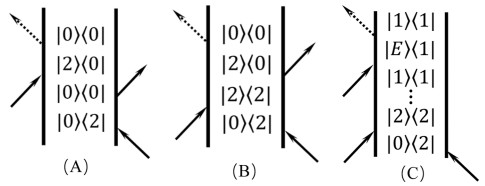

Figure 7. Double-sided Feynman diagrams of ground state bleaching (A), excited state emission (B), and ESA (C). $|0\rangle$, $|1\rangle$, and $|2\rangle$ represent the states of S_0, S_1, and S_2. $|E\rangle$ indicates the S_n excited state.

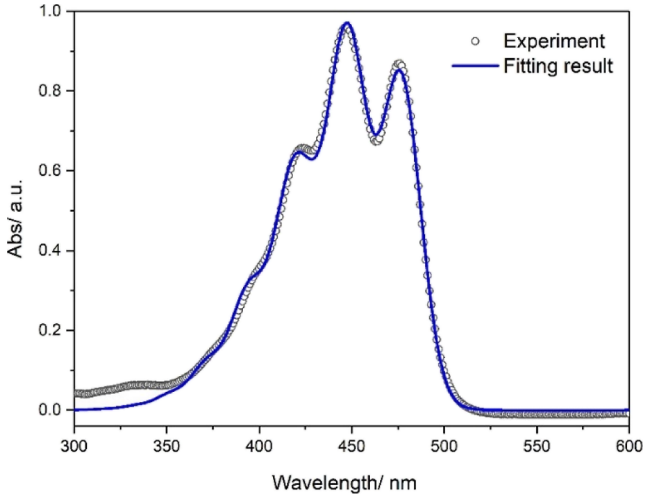

Figure 8. Experimentally steady (open circle) and theoretically linear (solid line) absorption spectra. Three vibrational modes are necessary to fit the experimental absorption well. The parameters for simulation are displayed in Table 2.

Figure 4, open circle is kinetic signal of lutein with 100 fs step, blue curve is fitted result based on Scheme 1 and (D), (E), and (F) are the curves of population dynamics of three excited states N_{11}, N_{12}, and N_{13}, respectively, of eq S2 in supplement. In scheme 1 which models the excited-state dynamics of 480 nm excitation, a short lifetime of ~106 fs of S_2 is observed and the other lifetimes of three branches around S_1 are found 2.8, 12, and 49 ps for S_{11}, S_{12}, and S_{13} excited state. As previously discussed, 2.8 and 12 ps originate from hot-S_1 and S_1 excited states respectively.[45] The 49 ps long lifetime component in our experiment seems in full agreement with the assignment of previously reported S* or $S^{\ddagger}$ state. However, both the facts that S* state is located above S_1 and the $S^{\ddagger} \rightarrow S_n$ is the red shoulder of $S_1 \rightarrow S_n$ band are inconsistent with our situation. We exclude the assignments of S_{13} to S* or $S^{\ddagger}$ state. Instead, we suggest that the longer lifetime component is produced by pair of triplets in analogy with the previous report. In Table 2, the relaxation rates of k_6 and k_7 are almost zero that means the transitions between S_{12} and S_{13}, S_{13}, and S_0 are forbidden and S_{13} may not have the same property as S_0 and S_{12}. Based on the analysis, we rebuild the excited-state relaxation of scheme 1 for 480 nm excitation, as exhibited in Figure 5. After the lowest absorption band of the S_2 state is excited by two pulses of 480 nm in the MTG experiment, it decays in 106 fs to form hot-S_1 and S_1 states. Then, the hot-S_1 further relaxes in 2.8 ps to produce the S_1 and triplet T states where the transition rate to T state is twice as fast as to S_1 state. The T state is strongly exchange-coupled and bound with S_1. The binding energy is estimated to come from two initial photons which will lead to less vibrational levels of hot-S_1 and S_1 states and a narrower ESA band.[43]

The dynamics of 380 nm excitation probed at 535 and 494 nm were fitted globally to visualize the evolution of the excited

Table 1. Gaussian Decomposition of ESA of Lutein in Ethanol Excited by Low- and High-Energy with Different Time-Delays

	3 ps			6 ps			10 ps			20 ps		
Ex/nm	peak/nm	fwhm/nm	$\frac{I_{Sh}}{I_{Max}}$	peak/nm	fwhm/nm	$\frac{I_{Sh}}{I_{Max}}$	peak/nm	fwhm/nm	$\frac{I_{Sh}}{I_{Max}}$	peak/nm	fwhm/nm	$\frac{I_{Sh}}{I_{Max}}$
480	536	22.8	0.47	537	45.1	0.32	536		0.34	537	26.8	0.27
	513	18.0		513	18.5		513	18.0		507	19.0	
	502	10.2		502	9.4		502	9.5				
380	531	42.5	0.60	534	34.5	0.67	533	33.1	0.65	535	45.1	0.8
	494	35.3		499	39.6		498	35.8		494	27.8	

https://doi.org/10.1021/acsomega.2c06371
ACS Omega 2022, 7, 48250−48260

Table 2. Rate Constant of Three Scheme Models and the Unit of Rate Constant is ps^{-1}

Scheme	k_1	k_2	k_3	k_4	k_5	k_6	k_7	k_8	k_9
1	6.01	3.28	0.122	0.148	0.281	0.0001	0	0.1287	0.0249
2	1.473	0.390	0.0855	0.0791					
3	2.562	2.328	0.1524	0.1525					

Table 3. Parameters Used in the Calculation of Steady Absorption Spectra and Non-Linear Vibrational Signal

Δ/cm^{-1}	Λ/cm^{-1}	λ/cm^{-1}	τ/fs	ω_0/nm	s_1	ν_1/cm^{-1}	s_2	ν_2/cm^{-1}	s_3	ν_3/cm^{-1}
468	16.7	38.5	167	433	0.677	1133	0.599	1600	0.118	3216
Δ/cm^{-1}	Λ/cm^{-1}	λ/cm^{-1}	τ/fs							
$\omega_{0\to2}$/nm	$\omega_{1\to n}$/nm	Γ_1	Γ_2	s_1	ν_1/cm^{-1}	s_2	ν_2/cm^{-1}	s_3	ν_3/cm^{-1}	
435	536	0	0	0.677	1126	0.599	1346	0.118	3281	
432	536	0	0	0.677	1166	0.599	1324	0.118	3243	

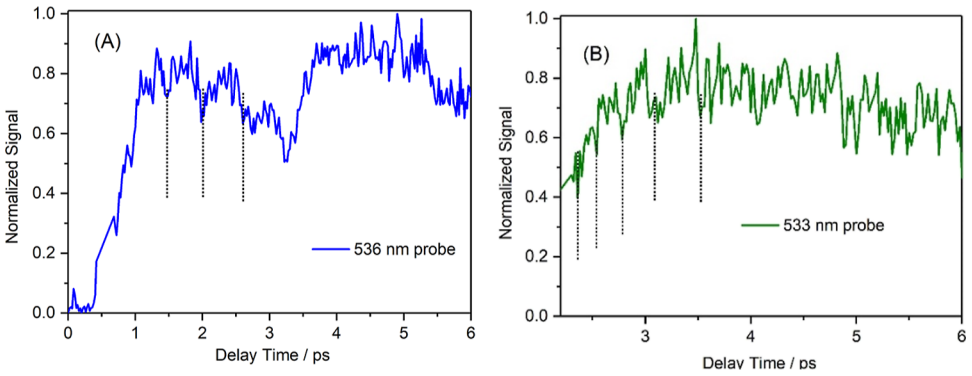

Figure 9. MTG kinetic signal of 480 nm excitation at 536 nm probe (A) and 380 nm excitation at 533 nm probe (B) with a 20 fs step. The coherent spike of each curve has been truncated for clarity. The dotted line is the period of the quantum beat.

states based on the relaxation Schemes 2 and 3 in Figure 3. Dissimilar to 480 nm excitation, three excited states are required enough to achieve a satisfactory fit of all kinetics of lutein in ethanol. The results in Figure 6 indicate that there is not any long lifetime component when the lutein is excited by high-energy side of the S_2 band. Comparing the fitted parameters in Table 2 (Scheme 2 and Scheme 3), the S_x state of Scheme 3 seems equivalent to S_1 as a result of $k_1 \approx k_2$ and $k_3 \approx k_4$. However, the equivalence between k_3 and k_4 will lead to no solution of the S_x population equation (eq S6) due to the fraction of (k_3-k_4) on the denominator. Therefore, we abandon the Scheme 3 and adopt Scheme 2 to describe the kinetics of lutein of 380 nm excitation. In contrast to 106 fs lifetime of S_2 state in Scheme 1, we observe a long-time scale of 536 fs of S_2 in Scheme 2 which can be explained in terms of vibrational relaxation. Besides the relatively long-time decay of S_2 state, the kinetics in Scheme 2 exhibits another two lifetimes of 14 and 14.9 ps corresponding S_x and S_1 state. Approximately, the S_x state can be decided on the basis of its decay properties. If it decays in the same time scale as S_1, it likely comes from the S_1 state, but if it has a lifetime markedly longer than the S_1 state, it may have its origin in S* state or triplet state. In the Scheme 2 model, although the relaxation time (14 ps) of S_x is much longer than the counterpart S_{11} in Scheme 1 (2.8 ps), we also here assign S_x to the hot-S_1 state for this time-delay is not long enough to regard S_x as S* or triplet.

By reference to the literature that suggested photo-isomerization of the carotenoid molecule,[46] we suppose a structural change in lutein that takes place following both low and high-energy excitation of two initial photons in this experiment. The high-energy excitation promotes an extremely small but non-zero structural change from the all-trans to the cis configuration in S_2 that will gradually restore to all-trans structure within the long lifetime (536 fs). The entire recovery of molecular structure in S_2 state improves the opportunity of a pure configuration in hot-S_1 upon the internal conversion from S_2 to S_1. This pure configuration in hot-S_1 demonstrates an extension of decay time, broader ESA band of $S_1 \to S_n$ and high $\frac{I_{Sh}}{I_{Max}}$ ratio comparing with 480 nm excitation. With the suggestion of photo-isomerization of S_2 discussed previously, the twisting structure in S_2 state of lutein molecule induced by two low-energy pulses cannot restore within the short lifetime (106 fs) of S_2 state, which will evolve into a hot-S_1 state of mixed configuration. The mixture of all-trans and the cis configuration has a critical participation in the formation of carotenoid triplet.

4.4. Vibrational Relaxation. The MTG signal of lutein solution in our experiment usually contains both population (non-oscillatory) dynamics and vibrational (oscillatory) relaxation. The former combing global fitting has been used to investigate the excited-state decay shown in the previous sections of this study. To explore the vibrational coherence, the population contribution in the form of exponential decay should be subtracted from the MTG signal. The residual signal then contains only the oscillatory contribution. Actually, the details of this vibrational residual are associated to several other factors such as the solvent, the excitation wavelength, and delay time. Therefore, we introduce the third-order nonlinear response function which integrates electronic states, solvent effects, and vibrational modes into a line-shape

https://doi.org/10.1021/acsomega.2c06371
ACS Omega 2022, 7, 48250−48260

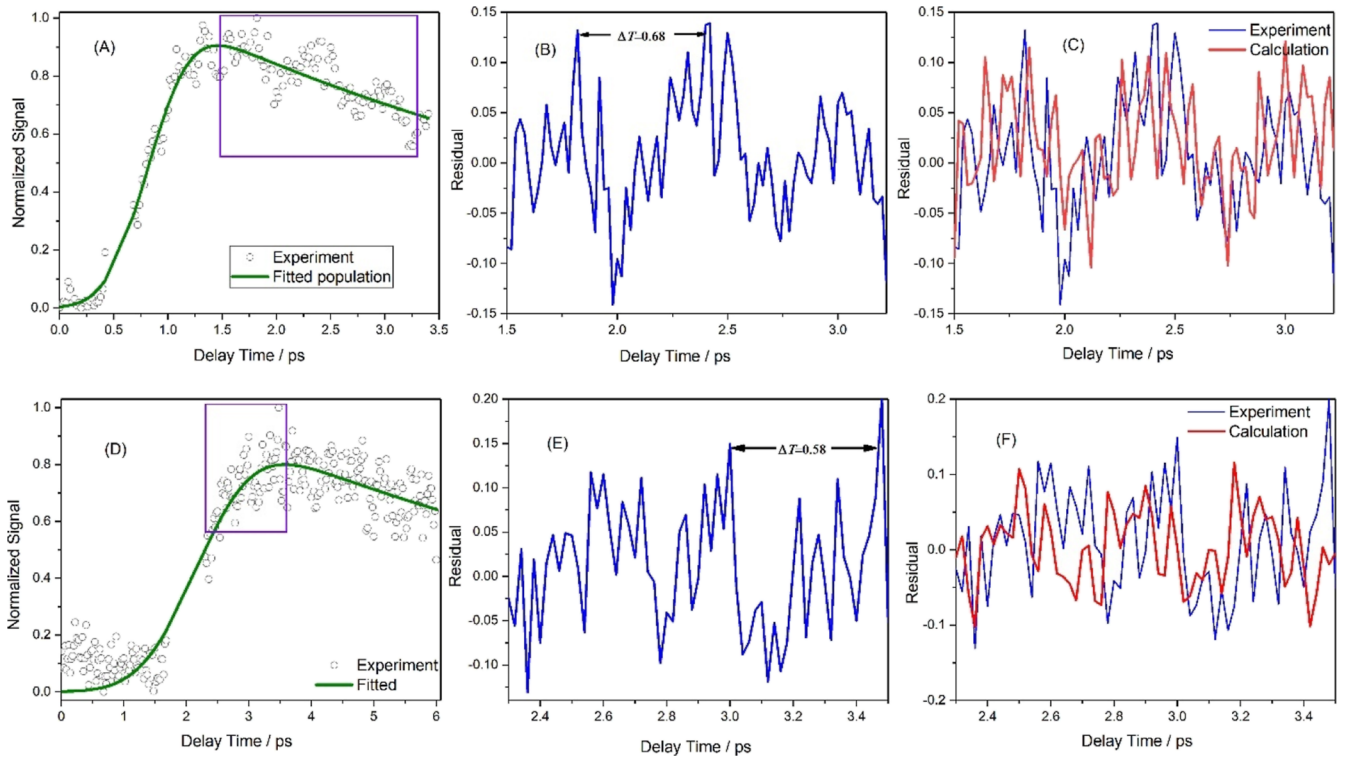

Figure 10. Kinetic trace in initial time of MTG (open circles) probed at 536 of 480 nm excitation (A) and 533 of 380 nm excitation (D). The traces are fitted with one exponential curve (green solid line, decay time is 5.6 and 9.58 ps for 480 and 380 excitations, respectively). By subtracting the exponential curves from the trace residual oscillations are obtained (B,E), which are simulated with non-linear signal of eq 4 based on response function [(C) for 480 nm excitation, (F) for 380 nm excitation]. The experiment results indicate that the beat signal from 480 nm excitation is more obvious that 380 nm excitation.

function to simulate the residual signal and to investigate the vibrational coherence.

The experimentally measured steady absorption of lutein in ethanol and the relative theoretical spectrum is demonstrated in Figure 8, and the parameters are shown in Table 3. The distinct vibrational profile of S_2 state in steady-absorption spectrum are matched well with the calculation of three vibrational modes with frequency at 1133, 1600, and 3216 cm^{-1}. The first two modes ν_1 and ν_2 have been observed before in frequency-domain Raman scattering from C−C stretching and C═C stretching vibration. The Huang−Rhys factors of the two modes having the values of 0.677 for ν_1 and 0.599 for ν_2 indicate that the structural changes in S_2 are greatly caused by these two vibrational modes. Significantly, the fitted result presented here reveals a third extraordinary high-frequency vibrational mode of 3216 cm^{-1} that should be assigned to O−H valence vibrations in the ionone rings of the molecule.[47] Although the Huang−Rhys of this high-frequency mode is small, it is essential in the fitting of steady spectra and is important in the non-linear signal where the molecular configuration changes due to the two photons' excitation.

For the sake of profound study of the coherently vibrational coupling of lutein in solution, a further MTG probe with a shorter time period of 20 fs in the time scale of 0−6 ps was carried out. The coherent oscillations with a period of a few tens of femtoseconds are clearly observed along the $-k_1 + k_2 + k_3$ direction in Figure 9. The kinetics of the time-resolved MTG in Figure 9 reveals a quantum beat that occurs about in the first 2 ps.[48] The kinetics trace within 6 ps of the lutein is fitted for dynamics by one-exponential function with decay constants 5.6 ps for 480 nm excitation (Figure 10A) and 9.58 ps for 380 nm excitation (Figure 10D). The residuals obtained by the subtracting the fitted exponential functions (green curves) from the transient kinetics signal (open circles) exhibit the short-lived quantum beats (Figure 10B,E). In pursuit of measuring the impact of the three observed vibrations on the dynamics of the excited-state decay, we made use of eq 6 to create a calculation of the nonlinear signal excluding the population dynamics to fit the experimental residuals. The comparing residual signals are exhibited in Figure 10C,F.

Generally, the appearance of beat reveals the quantum coherence originating from the superposition of electronic, vibrational states.[49] In our experiments, two initial laser pulses create a coherent superposition of quantum states, which gives rise to the quantum coherence and associated quantum beating signal. The likely source of the high-frequency beats in Figure 10 is a coherence between two vibrational modes.[50] The energy differences between the C−C stretching mode and C═C mode are 220 and 158 cm^{-1} for 480 and 380 nm excitation respectively shown in Table 3. The average beat period observed here in Figure 10B,E of ∼0.6 ps corresponds 55 cm^{-1} inconsistent with the difference of two vibrational modes (ν_1, ν_2). In order to take a deep study into the relationship between vibrational modes and quantum beating, we changed the three vibrational frequencies in calculating the non-linear signal. The resulted beat shown in supplement (Figure S4) illustrates a fact that the highest frequency mode (ν_3) is playing a critical role in quantum-beat frequency of the coherent vibration. Here, the quantum coherences include three types, electronic coherence between electronic states on different electronic potential energy surface, vibrational coherence between vibrational state, and vibronic coherence between excited vibronic states of

https://doi.org/10.1021/acsomega.2c06371
ACS Omega 2022, 7, 48250−48260

different molecule.[49] Therefore, we assume that the source of beating of ~0.6 ps period (Figure 10B,E) originates from the second type of coherently vibrational coupling of ν_1 and ν_3 or ν_2 and ν_3, that may be involved in the formation of the triplet state in Figure 5.

We conclude that after lutein is excited into S_2 state by two spatially and temporally overlapped pulses, molecular configuration mainly ascribed to C−C and C═C mode undergoes a different vibrational relaxation due to different excitation energies. According to the tendency of photo-isomerization, the O−H valence also has an opportunity to twist from the all-trans to cis configuration in the excited state and the twisting degree depends on the excited energy. For all-*trans*-*β*-carotene, the photo-isomerization has been detected by the optical Kerr effect and the structural recovering time is about 250 fs.[51] In our case of 480 nm excitation, the fitted lifetime of S_2 state is 106 fs, and that is not long enough to restore the molecular structure from cis to all-trans. As a result, upon internal conversion of $S_2 \rightarrow S_1$, a mixture of different molecular configurations is formed in the hot-S_1 that will be a key to generate a long-time triplet next. The beat associated with the triplet state may related to the vibrational coherence between different vibration modes. While for 380 nm excitation, the full recovery in the long-decay time (536 fs) of vibrational cooling of S_2 state makes a pure configuration decay to hot-S_1 state that will directly relax to the S_1 state. Our findings may open the door to resolve the relaxation dynamics of carotenoids in solution and in natural light-harvesting systems.

5. CONCLUSIONS

The MTG signals from lutein dissolved in ethanol have been measured in order to investigate the excitation-energy dependence of excited-state dynamics and vibrational relaxation. The experimental ESAs upon 380 and 480 nm excitation both exhibit a main peak corresponding to $S_1 \rightarrow S_n$ transition and a blue-wavelength shoulder that is called the S* state previously. Based on global fitting, three components (49, 12, and 2.8 ps) are derived from the signal of 480 nm excitation corresponding to the lifetime of the triplet, S_1, and hot-S_1 state. While for 380 nm excitation, two species with a similar time-scale of ~14 ps are observed which are also assigned to S_1 and hot-S_1 state. Additionally, the $S_2 \rightarrow S_1$ internal conversion time is extended from 106 to 536 fs when the excitation wavelength going from 480 to 380 nm, as a result of vibrational coherence and recovery of photoinduced deformation of molecular structure on the S_2 state. In the transient signal, quantum beat is observed which is investigated further by the time integration of the response functions. The simulation of steady and TA indicates that three vibrational modes (ν_1: C−C stretching, ν_2: C═C stretching, and ν_3: O−H valence) are involved, in which vibrational coherent of low and high modes (ν_1 and ν_3 or ν_2 and ν_3) is responsible for the high-frequency beat. The more distinguishable beat signal of 480 nm excitation than 380 nm excitation may imply the participation of the vibrational coherence occurring between different molecular configuration in hot-S_1 that is absent in the transient signal of 380 nm excitation due to the pure configuration.

Summarily, it is assumed that the excitation at low or high edge of S_2 band by two pulse pumping results in molecular distortion (from all-trans to cis) leading to a structural change in S_2 state. Short-time vibrational relaxation and decay (<300 fs) of the S_2 state induces a mixed configuration (all-trans and cis) in hot-S_1, which is the critical condition to evolve a coupling triplet as well as a quantum beat. The findings can explain that a pure configuration of hot-S_1 state has no contribution of long life-time state to a TA spectrum.[41] The results will help to promote the research of energy transfer and photoprotection mechanism of carotenoids in photosynthesis, and will be instructive for understanding of excitation-dependent triplet states in photoelectric conversion of materials.

■ ASSOCIATED CONTENT

Supporting Information

The Supporting Information is available free of charge at https://pubs.acs.org/doi/10.1021/acsomega.2c06371.

MTG signal of ethanol, Gaussian decomposition of excited state absorption, raw kinetical trace of the MTG signal from 480 and 380 nm excitation, simulated quantum beat generated by coherent vibrations of three modes, rate equations for schemes 1 and 2, and convolution of instrument response function and exponential decay (PDF)

■ AUTHOR INFORMATION

Corresponding Author

Lilin Jiang − *Office of Academic Research, Hezhou University, Hezhou, Guangxi 542899, China*; Email: jianglilin2009@163.com

Authors

Liping Lu − *College of Science, Nanjing Agricultural University, Nanjing, Jiangsu 210095, China*; orcid.org/0000-0002-8099-2657

Yunfei Song − *National Key Laboratory of Shock Wave and Detonation Physics, Institute of Fluid Physics, China Academy of Engineering Physics, Mianyang, Sichuan 621900, China*

Weilong Liu − *Department of Physics, Harbin Institute of Technology, Harbin, Heilongjiang 150080, China*

Complete contact information is available at: https://pubs.acs.org/10.1021/acsomega.2c06371

Notes

The authors declare no competing financial interest.

■ ACKNOWLEDGMENTS

The authors gratefully acknowledge the financial support of this research by the Fundamental Research Funds for the Central Universities, Nanjing Agricultural University (Grant No. XUEKEN2022033), Guangxi Natural Science Foundation (Grant No.2018GXNSFAA294063), and the Professional Foundation of Hezhou University (Grant No. HZUJS202006).

■ REFERENCES

(1) Christensen, R. L.; Galinato, M. G.; Chu, E. F.; Howard, J. N.; Broene, R. D.; Frank, H. A. Energies of low-lying excited states of linear polyenes. *J. Phys. Chem. A* **2008**, *112*, 12629−12636.

(2) Tavan, P.; Schulten, K. Electronic excitations in finite and infinite polyenes. *Phys. Rev. B: Condens. Matter Mater. Phys.* **1987**, *36*, 4337−4358.

(3) McNulty, H. P.; Byun, J.; Lockwood, S. F.; Jacob, R. F.; Mason, R. P. Differential effects of carotenoids on lipid peroxidation due to membrane interactions: X-ray diffraction analysis. *Biochim. Biophys. Acta* **2007**, *1768*, 167−174.

(4) Cogdell, R. J.; Isaacs, N. W.; Freer, A. A.; Howard, T. D.; Gardiner, A. T.; Prince, S. M.; Papiz, M. Z. The structural basis of light-harvesting in purple bacteria. *FEBS Lett.* **2003**, *555*, 35−39.
(5) Frank, H. A.; Bautista, J. A.; Josue, J. S.; Young, A. J. Mechanism of nonphotochemical quenching in green plants: energies of the lowest excited singlet states of violaxanthin and zeaxanthin. *Biochemistry* **2000**, *39*, 2831−2837.
(6) Young, A. J.; Frank, H. A. Energy transfer reactions involving carotenoids: quenching of chlorophyll fluorescence. *J. Photochem. Photobiol., B* **1996**, *36*, 3−15.
(7) Frank, H. A.; Cogdell, R. J. Carotenoids in photosynthesis. *Photochem. Photobiol.* **1996**, *63*, 257−264.
(8) Polívka, T.; Sundström, V. Ultrafast dynamics of carotenoid excited States-from solution to natural and artificial systems. *Chem. Rev.* **2004**, *104*, 2021−2072.
(9) Hashimoto, H.; Yanagi, K.; Yoshizawa, M.; Polli, D.; Cerullo, G.; Lanzani, G.; De Silvestri, S.; Gardiner, A. T.; Cogdell, R. J. The very early events following photoexcitation of carotenoids. *Arch. Biochem. Biophys.* **2004**, *430*, 61−69.
(10) Kosumi, D.; Fujiwara, M.; Fujii, R.; Cogdell, R. J.; Hashimoto, H.; Yoshizawa, M. The dependence of the ultrafast relaxation kinetics of the S(2) and S(1) states in beta-carotene homologs and lycopene on conjugation length studied by femtosecond time-resolved absorption and Kerr-gate fluorescence spectroscopies. *J. Chem. Phys.* **2009**, *130*, 214506.
(11) Kohler, B. E.; Samuel, I. D. W. Experimental determination of conjugation lengths in long polyene chains. *J. Chem. Phys.* **1995**, *103*, 6248−6252.
(12) Zhang, J.; Inaba, T.; Watanabe, Y.; Koyama, Y. Excited-state dynamics among the 1Bu+, 1Bu− and 2Ag− states of all-trans-neurosporene as revealed by near-infrared time-resolved absorption spectroscopy. *Chem. Phys. Lett.* **2000**, *332*, 351−358.
(13) Fujii, R.; Inaba, T.; Watanabe, Y.; Koyama, Y.; Zhang, J. Two different pathways of internal conversion in carotenoids depending on the length of the conjugated chain. *Chem. Phys. Lett.* **2003**, *369*, 165−172.
(14) Polívka, T.; Sundström, V. Dark excited states of carotenoids: Consensus and controversy. *Chem. Phys. Lett.* **2009**, *477*, 1−11.
(15) Andersson, P. O.; Gillbro, T. Photophysics and dynamics of the lowest excited singlet state in long substituted polyenes with implications to the very long-chain limit. *J. Chem. Phys.* **1995**, *103*, 2509−2519.
(16) Gradinaru, C. C.; Kennis, J. T. M.; Papagiannakis, E.; van Stokkum, I. H. M.; Cogdell, R. J.; Fleming, G. R.; Niederman, R. A.; van Grondelle, R. An unusual pathway of excitation energy deactivation in carotenoids: singlet-to-triplet conversion on an ultrafast timescale in a photosynthetic antenna. *Proc. Natl. Acad. Sci. U.S.A.* **2001**, *98*, 2364−2369.
(17) Papagiannakis, E.; Kennis, J. T.; van Stokkum, I. H.; Cogdell, R. J.; van Grondelle, R. An alternative carotenoid-to-bacteriochlorophyll energy transfer pathway in photosynthetic light harvesting. *Proc. Natl. Acad. Sci. U.S.A.* **2002**, *99*, 6017−6022.
(18) Khan, T.; Litvín, R.; Šebelík, V.; Polívka, T. Excited-State Evolution of Keto-Carotenoids after Excess Energy Excitation in the UV Region. *Chemphyschem* **2021**, *22*, 471−480.
(19) Larsen, D. S.; Papagiannakis, E.; van Stokkum, I. H. M.; Vengris, M.; Kennis, J. T. M.; van Grondelle, R. Excited state dynamics of β-carotene explored with dispersed multi-pulse transient absorption. *Chem. Phys. Lett.* **2003**, *381*, 733−742.
(20) Musser, A. J.; Maiuri, M.; Brida, D.; Cerullo, G.; Friend, R. H.; Clark, J. The Nature of Singlet Exciton Fission in Carotenoid Aggregates. *J. Am. Chem. Soc.* **2015**, *137*, 5130−5139.
(21) Chen, W.; Angelella, M.; Kuo, C. H.; Tauber, M. J. In *NanoScience + Engineering*; SPIE: San Diego, California, United States, 2012.
(22) Jailaubekov, A. E.; Song, S.; Vengris, M.; Cogdell, R. J.; Larsen, D. S. Using narrowband excitation to confirm that the S* state in carotenoids is not a vibrationally-excited ground state species. *Chem. Phys. Lett.* **2010**, *487*, 101−107.
(23) Llansola-Portoles, M. J.; Redeckas, K.; Streckaité, S.; Ilioaia, C.; Pascal, A. A.; Telfer, A.; Vengris, M.; Valkunas, L.; Robert, B. Lycopene crystalloids exhibit singlet exciton fission in tomatoes. *Phys. Chem. Chem. Phys.* **2018**, *20*, 8640−8646.
(24) Mimuro, M.; Akimoto, S.; Takaichi, S.; Yamazaki, I. Effect of Molecular Structures and Solvents on the Excited State Dynamics of the S2 State of Carotenoids Analyzed by the Femtosecond Up-Conversion Method. *J. Am. Chem. Soc.* **1997**, *119*, 1452−1453.
(25) Polívka, T.; Zigmantas, D.; Sundstrm, V.; Formaggio, E.; Bassi, R. Carotenoid S 1 State in a Recombinant Light-Harvesting Complex of Photosystem II. *Biochemistry* **2002**, *41*, 439−450.
(26) Walla, P. J.; Linden, P. A.; Ohta, K.; Fleming, G. R. Excited-State Kinetics of the Carotenoid S1 State in LHC II and Two-Photon Excitation Spectra of Lutein and β-Carotene in Solution: Efficient Car S1→Chl Electronic Energy Transfer via Hot S1 States? *J. Phys. Chem. A* **2002**, *106*, 1909−1916.
(27) Billsten, H. H.; Zigmantas, D.; Sundstrm, V.; Polvka, T. Dynamics of vibrational relaxation in the S 1 state of carotenoids having 11 conjugated C=C bonds. *Chem. Phys. Lett.* **2002**, *355*, 465−470.
(28) Buckup, T.; Hauer, J.; Möhring, J.; Motzkus, M. Multidimensional spectroscopy of beta-carotene: vibrational cooling in the excited state. *Arch. Biochem. Biophys.* **2009**, *483*, 219−223.
(29) Sugisaki, M.; Yanagi, K.; Cogdell, R. J.; Hashimoto, H. Unified explanation for linear and nonlinear optical responses in β -carotene: A sub- 20 fs degenerate four-wave mixing spectroscopic study. *Phys. Rev. B: Condens. Matter* **2007**, *75*, 155110.
(30) Kosumi, D.; Yanagi, K.; Nishio, T.; Hashimoto, H.; Yoshizawa, M. Excitation energy dependence of excited states dynamics in all-trans-carotenes determined by femtosecond absorption and fluorescence spectroscopy. *Chem. Phys. Lett.* **2005**, *408*, 89−95.
(31) Vauthey, E. Direct Measurements of the Charge-Recombination Dynamics of Geminate Ion Pairs Formed upon Electron-Transfer Quenching at High Donor Concentration. *J. Phys. Chem. A* **2000**, *105*, 340−348.
(32) Högemann, C.; Pauchard, M.; Vauthey, E. Picosecond transient grating spectroscopy: The nature of the diffracted spectrum. *Rev. Sci. Instrum.* **1996**, *67*, 3449−3453.
(33) Jiang, L.-l.; Liu, W. L.; Song, Y. F.; He, X.; Yang, Y. Q. Photoinduced intermolecular electron transfer and off-resonance Raman characteristics of Rhodamine 101/N,N-diethylaniline. *Chem. Phys.* **2013**, *429*, 12−19.
(34) Shaul, M.*Principles of Nonlinear Spectroscopy*; Oxford University Press: New York, 1995.
(35) Perlík, V.; Seibt, J.; Cranston, L. J.; Cogdell, R. J.; Hauer, J. Vibronic coupling explains the ultrafast carotenoid-to-bacteriochlorophyll energy transfer in natural and artificial light harvesters. *J. Chem. Phys.* **2015**, *142*, 212434.
(36) Lu, L.; Liu, Y.; Wei, L.; Wu, F.; Xu, Z. Structures and exciton dynamics of aggregated lutein and zeaxanthin in aqueous media. *J. Lumin.* **2020**, *222*, 117099.
(37) Seibt, J.; Pullerits, T. Combined treatment of relaxation and fluctuation dynamics in the calculation of two-dimensional electronic spectra. *J. Chem. Phys.* **2014**, *141*, 114106.
(38) Seibt, J.; Hansen, T.; Pullerits, T. 3D spectroscopy of vibrational coherences in quantum dots: theory. *J. Phys. Chem. B* **2013**, *117*, 11124−11133.
(39) Fourkas, J. T.; Trebino, R.; Fayer, M. D. The grating decomposition method: A new approach for understanding polarization-selective transient grating experiments. I. Theory. *J. Chem. Phys.* **1992**, *97*, 78−85.
(40) Kosumi, D.; Kusumoto, T.; Fujii, R.; Sugisaki, M.; Iinuma, Y.; Oka, N.; Takaesu, Y.; Taira, T.; Iha, M.; Frank, H. A.; Hashimoto, H. Ultrafast S 1 and ICT state dynamics of a marine carotenoid probed by femtosecond one- and two-photon pump-probe spectroscopy. *J. Lumin.* **2011**, *131*, 515−518.
(41) Niedzwiedzki, D. M.; Sullivan, J. O.; Polívka, T.; Birge, R. R.; Frank, H. A. Femtosecond Time-Resolved Transient Absorption

https://doi.org/10.1021/acsomega.2c06371
ACS Omega 2022, 7, 48250−48260

Spectroscopy of Xanthophylls. *J. Phys. Chem. B* **2006**, *110*, 22872−22885.
(42) Kosumi, D.; Kusumoto, T.; Fujii, R.; Sugisaki, M.; Iinuma, Y.; Oka, N.; Takaesu, Y.; Taira, T.; Iha, M.; Frank, H. A.; Hashimoto, H. Ultrafast excited state dynamics of fucoxanthin: excitation energy dependent intramolecular charge transfer dynamics. *Phys. Chem. Chem. Phys.* **2011**, *13*, 10762−10770.
(43) Saccon, F.; Durchan, M.; Radek, K.; Ondřej, P.; Alexander, V. R.; Tomáš, P. Spectroscopic Properties of Violaxanthin and Lutein Triplet States in LHCII are Independent of Carotenoid Composition. *J. Phys. Chem. B* **2019**, *123*, 9312−9320.
(44) Billsten, H. H.; Bhosale, P.; Yemelyanov, A.; Bernstein, P. S.; Polívka, T. Photophysical properties of xanthophylls in carotenoproteins from human retinas. *Photochem. Photobiol.* **2003**, *78*, 138−145.
(45) Billsten, H. H.; Pan, J.; Sinha, S.; Pascher, T.; Sundstr, M. V.; Polívka, T. Excited-state processes in the carotenoid zeaxanthin after excess energy excitation. *J. Phys. Chem. A* **2005**, *109*, 6852−6859.
(46) de Weerd, F. L.; Stokkum, I. H. M.; Grondelle, R. Subpicosecond dynamics in the excited state absorption of all-trans-b-Carotene. *Chem. Phys. Lett.* **2002**, *354*, 38−43.
(47) Davis, J. A.; Cannon, E.; Van Dao, L.; Hannaford, P.; Quiney, H. M.; Nugent, K. A. Long-lived coherence in carotenoids. *New J. Phys.* **2010**, *12*, 085015.
(48) Shutova, V. V.; Tyutyaev, E. V.; Churin, A. A.; Ponomarev, V. Y.; Maksimov, G. V. IR and Raman spectroscopy in the study of carotenoids of Cladophora rivularis algae. *Biophysics* **2016**, *61*, 601−605.
(49) Wang, L.; Allodi, M. A.; Engel, G. S. Quantum coherences reveal excited-state dynamics in biophysical systems. *Nat. Rev. Chem.* **2019**, 3, 477−490.
(50) Davis, J. A.; Cannon, E.; Van Dao, L. Long-lived coherence in carotenoids. *New J. Phys.* **2010**, *12*, 085015.
(51) Foggi, P.; Righini, R.; Torre, R.; Kamalov, V. F. Molecular dynamics of β-carotene in solution measured by subpicosecond transient optical Kerr effect. *Chem. Phys. Lett.* **1992**, *193*, 23−29.

https://doi.org/10.1021/acsomega.2c06371
ACS Omega 2022, 7, 48250−48260